

CIAO: Cache Interference-Aware Throughput-Oriented Architecture and Scheduling for GPUs

Jie Zhang*, Shuwen Gao[†], Nam Sung Kim[‡], and Myoungsoo Jung*

*School of Integrated Technology, Yonsei University, Korea

[†]Intel, USA

[‡]University of Illinois Urbana-Champaign, USA

Abstract—A modern GPU aims to simultaneously execute more warps for higher Thread-Level Parallelism (TLP) and performance. When generating many memory requests, however, warps contend for limited cache space and thrash cache, which in turn severely degrades performance. To reduce such cache thrashing, we may adopt cache locality-aware warp scheduling which gives higher execution priority to warps with higher potential of data locality. However, we observe that warps with high potential of data locality often incurs far more cache thrashing or interference than warps with low potential of data locality. Consequently, cache locality-aware warp scheduling may undesirably increase cache interference and/or unnecessarily decrease TLP.

In this paper, we propose Cache Interference-Aware throughput-Oriented (CIAO) on-chip memory architecture and warp scheduling which exploit unused shared memory space and take insight opposite to cache locality-aware warp scheduling. Specifically, CIAO on-chip memory architecture can adaptively redirect memory requests of severely interfering warps to unused shared memory space to isolate memory requests of these interfering warps from those of interfered warps. If these interfering warps still incur severe cache interference, CIAO warp scheduling then begins to selectively throttle execution of these interfering warps. Our experiment shows that CIAO can offer 54% higher performance than prior cache locality-aware scheduling at a small chip cost.

Keywords—GPGPU; thread-level parallelism; warp scheduling; interference;

I. INTRODUCTION

The hardware-based warp scheduler of modern GPUs aims to schedule as many warps as possible to its Stream Multi-processors (SMs) to increase TLP and thus performance [1]. Such warp scheduling, however, is not efficient for memory-intensive applications in which active warps collectively generate too many memory requests and thus contend for limited cache space [2], [3]. Prior work reports that such cache contention (or interference) frequently incurs cache thrashing and therefore severely degrades performances [4], [5], [6]. For example, our own experiment shows that a GPU can improve the geometric-mean performance of popular benchmark suites such as PolyBench [7], Mars [8] and

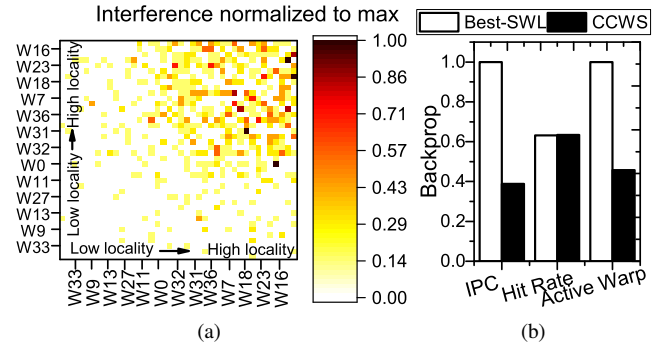


Figure 1: Backprop [9]: (a) cache interference and (b) performance, cache hit rate, and number of active warps of Best-SWL and CCWS.

Rodinia [9] by 89% when perfectly eliminating cache interference.

To reduce cache thrashing, various cache-aware warp scheduling techniques have been proposed (*e.g.*, [10], [11], [12]). These warp scheduling techniques aim to improve L1D cache hit rates and thus performance by identifying warps with high potential of data locality and then giving these warps a higher execution priority than other warps (*i.e.*, judiciously reducing TLP by throttling execution of warps with low potential of data locality). However, we observe that such warp scheduling techniques are often inefficient especially for memory-intensive applications with *irregular* cache access patterns due to two key reasons. First, cache accesses of active warps with high potential of data locality often severely interfere with one another. Consequently, scheduling warps simply based on their potential of data locality frequently increases cache interference with limited or even negative effect on improving cache hit rates. Second, it is undesirable to significantly reduce TLP in exchange for improved cache hit rates. That is, although throttling execution of such warps may improve cache hit rates, overall performance can be either marginally improved or even degraded.

To provide better insights on our aforementioned observations, we run Backprop [9] using a popular GPU

This paper is accepted by and will be published at 2018 International Parallel and Distributed Processing Symposium. This document is presented to ensure timely dissemination of scholarly and technical work.

model [13]. Then we analyze (1) which cache accesses of previously executed warps interfere with those of a currently executed warp and (2) how many cache misses of the currently executed warp are incurred by those of these previously executed warps in Figure 1a. This plot shows that a few warps with high potential of data locality (*i.e.*, W16, W23, and W18) also severely interfere with one another, incurring many unnecessary cache misses. We also consider two popular warp scheduling techniques: *Best-SWL* (*Best-Static-Wavefront-Limiting* scheduler) [12] and *CCWS* (*Cache-Conscious Wavefront Scheduling*) [12], and compare performance, cache hit rate, and number of active warps of these two scheduling techniques in Figure 1b. *Best-SWL* and *CCWS* aim to throttle execution of warps based on the best limitation value and potential of data locality determined by profiling and runtime techniques, respectively. This plot shows that both *Best-SWL* and *CCWS* accomplish similar cache hit rates, but *Best-SWL* performs much better than *CCWS* as it reduces TLP less.

In this paper, tackling the aforementioned limitation of data locality-aware scheduling, we propose **Cache Interference-Aware throughput-Oriented (CIAO)** on-chip memory architecture and warp scheduling which exploit unused shared memory space and take insight opposite to cache locality-aware scheduling. Specifically, we make the following contributions.

First, we demonstrate that cache locality-aware scheduling, which gives higher execution priority to warps with *higher* potential of data locality than warps with *lower* potential of data locality, often undesirably increases cache interference and/or unnecessarily decreases TLP. Second, we propose CIAO on-chip memory architecture that can adaptively redirect as many memory requests of interfering warps as possible to unused shared memory space, cost-effectively isolating memory requests of interfering warps from those of interfered warps. This CIAO on-chip memory architecture alone can notably reduce cache interference without diminishing TLP, providing **32%** higher performance than *CCWS*. Nonetheless, we may not be able to redirect every memory request of these interfering warps due to the limited unused shared memory space, and these warps may still incur severe cache interference. To efficiently handle such a case, we then propose CIAO warp scheduling which begins to selectively throttle execution of these interfering warps (*i.e.*, giving lower priority to warps with *high* potential of data locality), whereas *CCWS* throttles execution of warps with *low* potential of data locality. Lastly, the synergistic integration of CIAO on-chip memory architecture and warp scheduling offers **54%** higher performance than *CCWS*, because it significantly reduces L1D cache interference while keeping higher TLP.

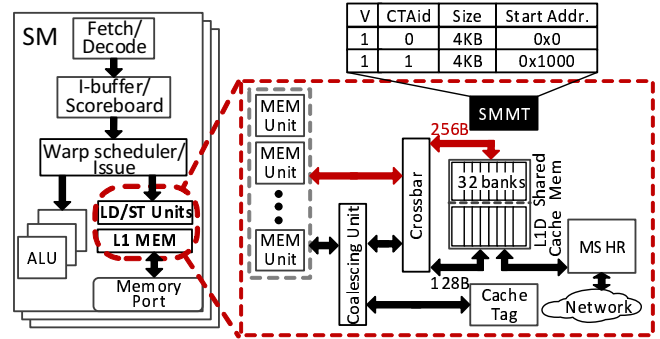


Figure 2: GPU SM architecture.

II. BACKGROUND

A. GPU SM Architecture

Figure 2 illustrates a representative SM architecture where shared memory may share a single on-chip memory structure with L1D cache [1], [14]. The single on-chip memory structure consists of 32 banks with 512 rows, where 128 or 384 contiguous rows can be allocated to shared memory (*i.e.*, 16KB or 48KB) based on user configuration and the remaining are allocated as L1D cache [15]. While all 32 L1D cache banks operate in tandem for a single contiguous 32×4-byte (128-byte) L1D cache request, all 32 shared memory banks can be accessed independently and serve upto 32 shared memory requests in parallel. L1D cache buffers data from underlying memory and keeps a separate tag array to identify data hit. In such architecture, a L1D cache access is serialized. That is, tag array is accessed before the banks are accessed [16]. In contrast, as shared memory stores intermediate results generated by ALU for each Cooperative Thread Array (CTA) which is explicitly manipulated by programmers, it neither needs tags nor accesses data in underlying memory. Hence, there is no datapath between shared memory and L2 cache, and no cache write/eviction policies are applied in shared memory [1], [14]. In addition, to manage the shared memory space, each SM keeps an independent Shared Memory Management Table (SMMT) [17] where each CTA reserves one entry to store the size and base address of allocated shared memory.

B. Cache Interference

As many warps share small L1D cache, they often contend for the same cache line. Hence, cached data of an active warp are frequently evicted by cache accesses of other active warps. This phenomenon is referred to as *cache interference* which often changes supposedly a regular memory access pattern into an irregular one. Figure 3a depicts an example of how the cache interference worsens data locality in L1D cache, where warps W0 and W1 send memory requests to get data D0 and D4, respectively. However, since D0 and D4 are mapped to the same cache set S0, repeated memory

requests from W0 and W1 to get D0 and D4 keep evicting D4 and D0 at cycles (a), (b), (e), and (f). Unless the memory requests from W1 and W0 evicted D0 and D4, respectively, they should have been L1D cache hits. Such a cache hit opportunity is also called *potential of data locality*, which can be quantified by the frequency of re-referencing the same data unless cache interference occurs.

C. Potential of Data Locality Detection

To detect the potential of data locality described in Section II-B, we may leverage a Victim Tag Array (VTA) [12] where we store a Warp ID (WID) in each cache tag, as shown in Figure 3b. A WID in a cache tag is to track which warp brought current data in a cache line. When a memory request of a warp evicts data in a cache line, we first take (1) the address in the cache tag associated with the evicted data and (2) the WID of the warp evicting the data. Then we store (1) and (2) in a VTA entry which is indexed by the WID stored in the cache tag (*i.e.*, the WID of the warp which brought the evicted data in the cache line). When memory requests of an active warp repeatedly incur VTA hits, they exhibit potential of data locality.

III. ARCHITECTURE AND SCHEDULING

In this section, we overview CIAO (1) cache interference detection mechanism; (2) on-chip memory architecture and (3) warp scheduling, which can synergistically reduce cache thrashing without notably hurting TLP. We will describe their implementation details in Section IV.

A. Cache Interference Detection

As introduced in Section II-B, some warps incur more severe cache interference than other warps (*i.e.*, non-uniform cache interference). However, it is non-trivial to capture such non-uniform interference occurring during the execution of applications at compile time [18]. Thus, we need to determine severely interfering and interfered warps at runtime.

At run time, we may track severely interfered warps, leveraging a VTA structure (*cf.* Section II-C). A naïve way to determine severely interfering warps for each warp,

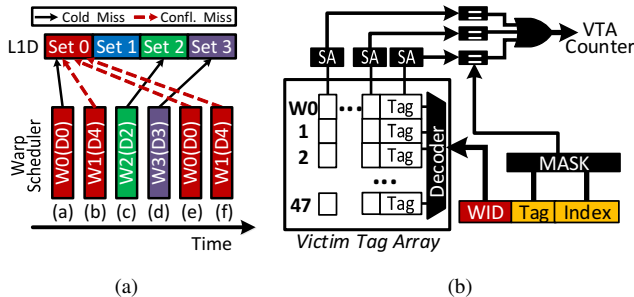


Figure 3: (a) An example of locality and interference and (b) VTA structure.

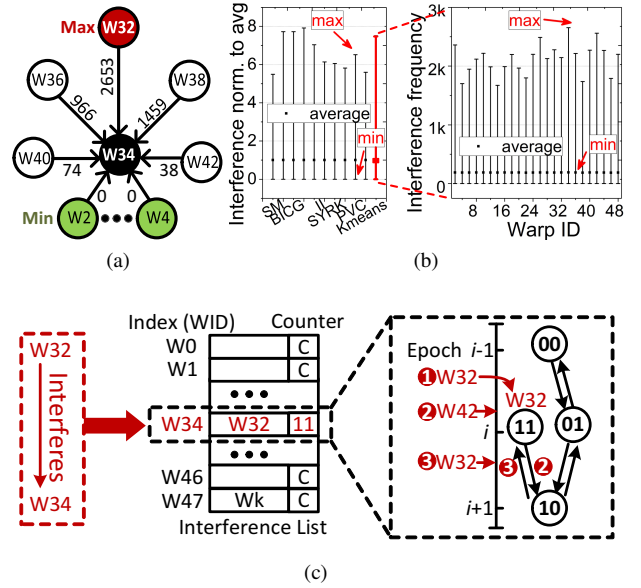


Figure 4: (a) Warps interfering with warp W34 and their interference frequency. (b) Min and max interference frequencies experienced by each warp and each evaluated workload. (c) Interference detection example.

however, demands a high storage cost, because each warp needs to keep track of cache misses incurred by all other $n - 1$ warps. This in turn requires a storage structure with $n(n - 1)$ entries where n is the number of active warps per SM (*i.e.*, 48 warps). Searching for a cost-effective way to determine severely interfering warps, we exploit our following observation on an important characteristic of cache interference.

Figure 4a shows that W32 interferes with W34, more than two thousand times, whereas some warps (*e.g.*, W2) do not interfere with W34 at all in KMEANS [9]; we observe a similar trend on cache interference in all other benchmarks that we tested (*cf.* Figure 4b). Observing such an interference characteristic, we propose to track only the most recently and frequently interfering warp for each warp. This significantly reduces the storage cost required to track every interfering warp for each warp. Specifically, CIAO keeps a small memory structure denoted by *interference list* where each entry is indexed by the WID of a currently executed warp.

To track the most recently and frequently interfering warp for a currently executed warp, we may augment each list entry with a 2-bit saturation counter. Figure 4c illustrates how CIAO utilizes the counter to track an interfering warp. Suppose that a previously executed warp (W32) interfered with a currently executed warp (W34). That is, W32 is an interfering WID and W34 is an interfered WID. Subsequently, the interfering WID is stored in the list entry indexed by

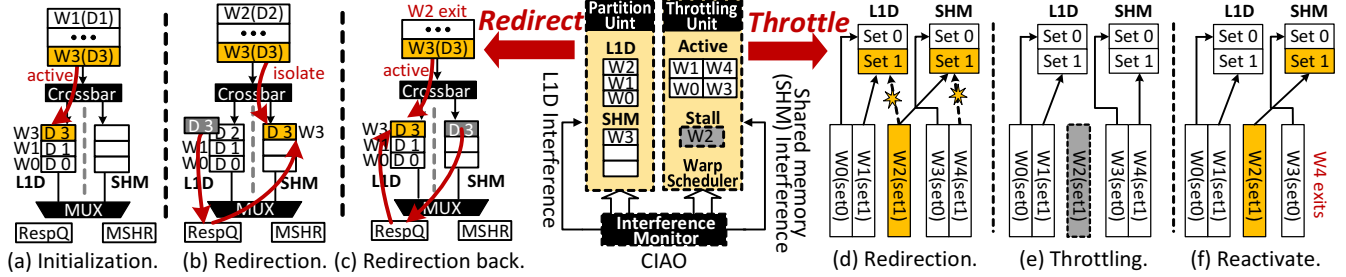


Figure 5: CIAO execution flow.

the interfered WID, and the counter in the list entry is set to 00; the interfering WID is provided by a VTA entry field that tracks which warp incurred the last eviction (*cf.* Section II-C).

Whenever W_{32} interferes with W_{34} (not shown in the figure), the counter is incremented by 1. Suppose that the counter has already reached 11 (1) at a given cycle. When another warp (W_{42}) interferes with warp W_{34} in a subsequent cycle, the counter is decremented by 1 (2). Then, if warp W_{32} interferes with W_{34} again, the counter is incremented by 1 (3). The interfering WID in the list entry is replaced with the most recent interfering WID only when its saturation counter is decreased to 00, so that the warp with most frequent cache interference can be kept in the interference list.

B. CIAO On-Chip Memory Architecture

An effective way to reduce cache interference is to isolate cache accesses of interfering warps from those of interfered warps after partitioning the cache space and allocating separate cache lines to the interfering warps. Prior work proposed various techniques to partition the cache space for CPUs (*e.g.*, [19], [20]). However, the size of L1D cache is insufficient to apply such techniques for GPUs, as the number of GPU threads sharing L1D cache lines is very large, compared with that of CPU threads. For example, only two or three cache lines can be allocated to each warp, if we apply a CPU-based cache partitioning technique to the L1D cache of GTX480. Such a small number of cache lines per warp can even worsen cache thrashing.

Meanwhile, we observe that programmers prefer L1D cache rather than shared memory for programming simplicity and the limited number of running GPU threads constrains the usage of shared memory, leading to a large fraction of shared memory unused (*cf.* F_{smem} of Table II in Section V-A). This agrees to prior work’s analysis [21], [22]. Exploiting such unused shared memory space, we propose to redirect memory requests of severely interfering warps to the unused shared memory space.

As there is no cache interference at the beginning of kernel execution, memory requests of all the warps are directed to

L1D cache, as depicted in Figure 5a. However, as the kernel execution progresses, cache accesses begin to compete one another to acquire specific cache lines in L1D cache. As the intensity of cache interference exceeds a threshold, CIAO determines severely interfering warps (*cf.* Section III-A). Subsequently, CIAO redirects memory requests of these interfering warps to unused shared memory space, isolating the interfering warps from the interfered warps in terms of cache accesses, as depicted in Figure 5b. This in turn can significantly reduce cache contentions without throttling warps (*i.e.*, hurting TLP). After the redirection, the memory requests are forwarded from L1D cache to shared memory but the data may already be present in the L1D cache (*cf.* W_3/D_3 in Figure 5b). To guarantee cache coherence between L1D cache and shared memory, single data copy needs to be exclusively stored in either shared memory or L1D cache. Such challenge can be addressed by migrating the data copy from L1D cache to shared memory, which may take the steps as follows: 1) a data miss signal would be raised for shared memory, 2) the data copy in L1D cache would be evicted to response queue, and 3) a new entry of MSHR would be filled with the pointer referring to the location of single data copy in the response queue. Later on, to fill the data miss, shared memory fetches data from response queue based on the location information recorded in MSHR. When CIAO detects significant decrease in cache contentions due to a change in cache access patterns or completion of execution of some warps, it redirects the memory requests of these interfering warps from shared memory back to L1D cache (*cf.* Figure 5c).

To exploit the unused shared memory space for the aforementioned purpose, however, there are two challenges. First, the shared memory has its own address space separated from the global memory, and there is no hardware support that translates a global memory address to a shared memory address. Second, the shared memory does not have a direct datapath to L2 cache and main memory [23]. That is, it always receives and sends data only through the register file. To overcome these limitations, we propose to adapt shared memory architecture as follows. First, we implement an address translation unit in front of shared memory to

translate a given global memory address to a local shared memory address. Second, we slightly adapt the datapath between L1D and L2 caches such that the shared memory can also access L2 cache when the unused shared memory space serves as cache.

C. CIAO Warp Scheduling

Although CIAO on-chip memory architecture can effectively isolate cache accesses of interfering warps from those of interfered warps, its efficacy depends on various run-time factors, such as the number of interfering warps and the amount of unused shared memory space. For example, the interfering warps end up thrashing the shared memory as well when the amount of unused shared memory space is insufficient to handle a large number of memory requests from the interfering warps in a short time period (cf. Figure 5d).

To efficiently handle such a case, we propose to throttle interfering warps *only* when it is not effective to redirect memory requests of interfering warps to the shared memory. Specifically, sharing the same cache interference detector used for CIAO on-chip memory architecture, CIAO monitors the intensity of interference at the shared memory at runtime. Once the intensity of interference at the shared memory exceeds a threshold, CIAO stalls the most severely interfering warp at the shared memory (e.g., W2 in Figure 5e). CIAO repeats this step until the intensity of interference at the shared memory falls below the threshold. As some warps complete their execution and subsequently the intensity of interference at the shared memory falls below the threshold, CIAO starts to reactivate the stalled warp(s) in the reverse order to keep high TLP and maximize the utilization of shared memory (cf. Figure 5f).

Note that CIAO warp scheduling shares the same interference detector with CIAO on-chip memory architecture, instead of keeping two separate interference detectors for L1D and shared memory, respectively. This is because isolated interfering warps do not compete L1D cache with warps that exclusively access L1D cache, and memory accesses of isolated interfering warps often interfere with one another. In other words, L1D cache and shared memory interferences do not affect each other. Hence, L1D cache and shared memory can share the same VTA array to detect interferences.

IV. IMPLEMENTATION

In this section, we present required GPU microarchitecture adaptations to implement the interference detector, on-chip memory architecture, and warp scheduling.

A. Cache Interference Detection

Estimation of cache interference. A level of cache interference experienced by a warp can be quantified by an Individual Re-reference Score (IRS) which can be expressed by:

$$IRS_i = \frac{F_{VTA-hits}^i}{N_{executed-inst}/N_{active-warp}} \quad (1)$$

where i is active warp number, $F_{VTA-hits}^i$ is the number of VTA hits for warp i , $N_{executed-inst}$ is the total number of executed instructions, and $N_{active-warp}$ is the number of active warps running on an SM, respectively. IRS_i represents VTA hits per instruction (i.e., intensity of VTA hits) for warp i . High IRS_i indicates warp i has experienced severe cache interference in a given epoch. Based on IRS_i , CIAO (1) decides whether it isolates warps interfering with warp i , (2) stalls these interfering warps, or (3) reactivates the stalled warps.

Decision thresholds. For these aforementioned three decisions we introduce two threshold values: (1) high-cutoff and (2) low-cutoff. IRS_i over high-cutoff indicates that warp i has experienced severe cache interference. Subsequently, CIAO decides to isolate or stall the warp that most recently and severely interfered with warp i . IRS_i below low-cutoff often indicates that warp i has experienced light cache interference and/or completed its execution. Then, CIAO decides to reactivate previously stalled warps or redirect memory requests of these warps back to L1D cache. As these two thresholds influence the efficacy of CIAO, we sweep these two values, evaluate diverse memory-intensive applications, and determine that high-cutoff and low-cutoff, which minimize cache interference and maximize performance, are 0.01 and 0.005, respectively. See Section V-E for our sensitivity analysis.

Epochs. As IRS_i changes over time, CIAO should track the latest IRS_i and compare it against high-cutoff and low-cutoff to precisely determine whether a warp needs to be isolated, stalled, or reactivated. However, the update of IRS_i calculation consumes more than 6 cycles, which can be on the critical path of performance. To this end, CIAO divides the execution time into high-cutoff

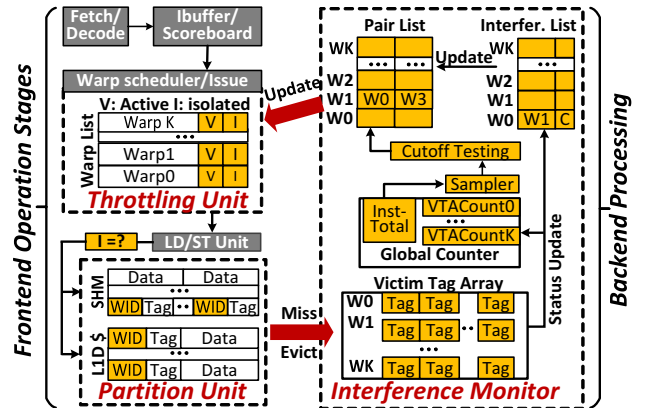


Figure 6: Microarchitecture adaptation for CIAO.

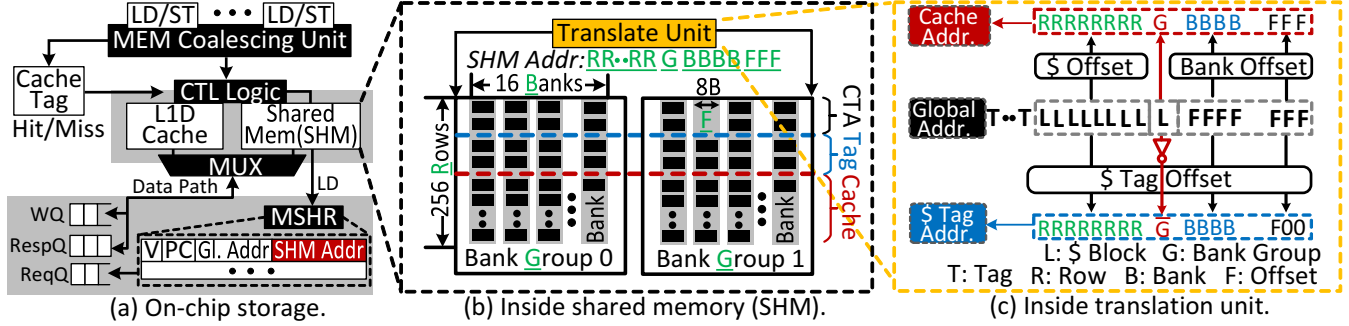


Figure 7: GPU on-chip memory structure adaptation.

and low-cutoff epochs, respectively. At the end of each high-cutoff (or low-cutoff) epoch, CIAO updates IRS_i and compares it against high-cutoff (or low-cutoff). The low-cutoff epoch should be shorter than the high-cutoff epoch because of the following reasons. As preserving high TLP is a key to improve GPU performance, CIAO attempts to minimize a negative effect of stalling warps by reactivating stalled warps as soon as these warps start not to notably interfere with other warps at runtime. To validate this strategy, we sweep high-cutoff and low-cutoff epoch values, evaluate diverse memory-intensive applications, and determine that the best high-cutoff and low-cutoff epoch values are every 5000 and 100 instructions, respectively. See Section V-E for our in-depth sensitivity analysis.

Microarchitecture support. Figure 6 depicts the necessary hardware, which is built upon the existing VTA organization [12], to implement a cache interference detector.

To capture different levels of cache interference experienced by individual warps, we implement a VTA-hit counter per warp and a total instruction counter per SM (VTAcount_{0-k} and Inst-total in the figure) atop a VTA. Each VTA-hit counter records the number of VTA hits for each warp, and the total instruction counter tracks the total number of instructions executed by a given SM (*i.e.*, $N_{executed-inst}$ in Eq.(1)). To compare IRS_i against high-cutoff and low-cutoff, we implement the cutoff testing unit which can be implemented by registers, a shifter, and simple comparison logic. Lastly, we implement the samplers to count the number of executed instructions and determine whether or not the end of a high-cutoff or low-cutoff epoch has been reached.

To manage the information related to tracking interfering warps for each warp, we implement the interference list. Each entry is indexed by WID of a given warp and stores a 6-bit WID of an interfering warp and a 2-bit saturation counter (C in the figure). When a VTA hit occurs, the corresponding entry of interference list is updated, as described in Section III-A. CIAO checks the interference list for warp i whenever it needs to isolate or stall an interfering warp based

on IRS_i . To facilitate this, we also augment a 1-bit active flag (V) and 1-bit isolation flag (I) with each ready warp entry in the warp list (*i.e.*, a component of warp scheduler). Using V and I bits, the warp scheduler can identify whether a given warp is in active ($V=1, I=0$), isolated ($V=1, I=1$), or stalled state ($V=0$).

We also implement a *pair list*. Each entry is indexed by the WID of a warp at the front of the warp list and composed of two fields to record which interfered warp triggered to redirect memory requests of the warp or stall the warp in the past. Suppose that warp i is at the front of the warp list. Based on WIDs from the first or second field of the entry indexed by warp i , CIAO checks IRS_k where k is the WID of the interfered warp that previously triggered to either redirect memory requests of warp i or stalling warp i . Then CIAO decides whether it reactivates warp i or redirects memory requests of warp i back to L1D cache based on IRS_k . For example, as W0 is severely interfered by W1, CIAO decides to redirect memory requests of W1 to unused shared memory space. Then W0 is recorded in the first field of the entry indexed by W1 and I associated with W1 is set, as depicted in Figure 6. Subsequently, W1 begins to send memory requests to the shared memory, but CIAO observes that W1 also severely interferes with W3 that sends its memory requests to the shared memory. As CIAO decides to stall W1, W3 is recorded in the second field of the entry indexed by W1 and V associated with W1 is cleared. When CIAO needs to reactivate W1 later, the second field of the pair list entry and V corresponding to W1 are cleared to inform the warp scheduler of the event that the warp is active. When CIAO needs to make W1 send its memory request back to L1D cache, the corresponding field in the pair list entry and I are cleared. See Section IV-C for more details on the pair list.

B. Shared Memory Architecture

Figure 7a and b illustrate CIAO on-chip memory architecture and its data placement layout, respectively.

Determination of unused shared memory space. One challenge to utilize unused shared memory space is that

shared memory is managed by programmers and the used amount of shared memory space varies across implementations of a kernel. To make CIAO on-chip memory architecture transparent to programmers, we leverage the existing SMMT structure to determine the unused shared memory space. When a CTA is launched, CIAO checks the corresponding SMMT entry to determine the amount of unused shared memory space (*cf.* Section II-A). Then, CIAO inserts a new entry in the SMMT with the start address and size of unused shared memory to reserve the space for storing 128-byte data blocks and tags.

Placement of tags and data. In contrast to L1D cache, shared memory does not have a separate memory array to accommodate tags [15]. In this work, instead of employing an additional tag array, we propose to place both 128-byte data blocks and their tags into the shared memory. This is to minimize the modification of the current on-chip memory structure architected to be configured as both L1D cache and shared memory. As shown in Figure 7b, we partition 32 shared memory banks into two bank groups and stripe a 128-byte data block across 16 banks within one bank group. Each 128-byte data block can be accessed in parallel since each shared memory bank allows 64-bit accesses [14]. Since a tag and a WID require only 31 bits ($= 25 + 6$ bits), two tags can be placed in a single bank which is different from banks storing the corresponding data blocks. Then 32 tags can be grouped together to better utilize a row of one bank group (*i.e.*, 16 banks). This design strategy, which puts a tag and the corresponding data block into two different bank groups, shuns bank conflicts and thus allows accesses of a tag and a data block in parallel. Furthermore, we only use the unused shared memory space as direct-mapped cache so that a pair of a 128-byte data block and the corresponding tag can be accessed with a single shared memory access.

Address translation unit. As shown in Figure 7b, we introduce a hardware address translation unit in front of shared memory to determine where a target 128-byte data block and its tag exist in the shared memory. In practice, a global memory address can be decomposed by cache-related information such as a tag, block index and byte offset. However, as the usage of shared memory can be varying based on the needs of each CTA, we put an 8-bit mask into the translation unit to decide how many rows will be used for each CTA at runtime. Figure 7c shows how our translation unit determines locations of a target data block and its tag; the data block address (of shared memory) consists of four fields, the byte offset (“F”), bank index (“B”), bank group (“G”), and row index (“R”), which are presented from LSB to MSB. Specifically, we have 8-byte rows per bank, 16 banks per group, two bank groups and 256 rows (at most), which in turn 3, 4, 1, and 8 bits for F, B, G and R, respectively. The remaining bits (16 bits in this example) are used as part of the tag. Note that our tags also contain 6-bit WID and 9-bit data block index as the number of cache lines required

can be greater than the number of rows.

In CIAO, one row within a bank group can hold 32 tags since a physical row per bank contains two tags. That is, the actual position of a tag can be indicated by 5 bits (*i.e.*, 1 F and 4 B bits), which are also used for the row index of the corresponding data block. To access a data block and the corresponding tag in parallel, G of the data block will be flipped and assigned to such tag’s 5 bits as a significant bit. The remaining R bits are assigned to the row index of the target tag. Note that, as shown in the figure, the start of index for both a data block and a tag can be rearranged by considering the data block and tag offset registers, which are used to adapt the unused shared memory size allocated for cache.

Datapath connection. When we leverage unused shared memory as cache, we need a datapath between shared memory and L2 cache. Since the shared memory is disconnected from the global memory in the conventional GPU, we need to adapt the on-chip memory structure, which is partitioned between L1D cache and shared memory, to share some resources of the L1D cache with the shared memory (*e.g.*, datapath to L2 cache, MSHR, etc.). As illustrated in Figure 7a, a multiplexer is implemented to connect the write queue (WQ) and response queue (RespQ) to either L1D cache or shared memory. The CIAO cache control logic controls the multiplexer based on the isolation flag bit (I) and the result of checking cache tags associated with accessing L1D cache or shared memory serving as cache. We also augment an extra field with each MSHR entry to store the shared memory address of a memory request from the aforementioned address translation unit. Once the shared memory issues a fill request after a miss, the request reserves one MSHR entry by filling in its global and translated shared memory addresses. If the response from L2 cache matches the global address recorded in the corresponding MSHR entry, the filling data can be directly stored in the shared memory based on the translated shared memory address.

Performance optimization and coherence. When CIAO redirects memory requests of an interfering warp from L1D cache to shared memory, the shared memory does not have any data. This can incur (1) performance degradation because of cold misses and (2) some coherence issues. To address these two issues, when CIAO needs to access the shared memory, the cache controller first checks the tag array of L1D cache. If a target data resides in L1D cache (not in shared memory), the L1D cache will evict the data directly to the response queue, which is used to buffer the fetched data from L2 cache and invalidate the corresponding cache line in L1D cache. Note that checking the tag array and accessing L1D cache are serialized as described in Section II-A. Meanwhile, the shared memory issues a fill request to MSHR, as the shared memory does not have the data yet. During this process, the target data will be directly fetch from the response queue to the shared memory (*cf.*

Algorithm 1: CIAO scheduling algorithm

```

1 i := getWarpToBeScheduled()
2 InstNo := getNumInstructions()
3 ActiveWarpNo := getNumActiveWarp()
4 if Warp(i).V == 0 and end of low cut-off epoch then
    /* Warp(i) is stalled */
    k := Pair_List[i][1]
    IRSk := VTAHit[k] / InstNo / ActiveWarpNo
    if IRSk > low-cut-off and Warp(k) needs executing then
        continue
    else
        Warp(i).V := 1
        Pair_List[i][1] := -1 // cleared
11 else if Warp(i).I == 1 and end of low cut-off epoch then
    /* Warp(i) redirects to access shared memory */
    k := Pair_List[i][0]
    IRSk := VTAHit[k] / InstNo / ActiveWarpNo
    if IRSk > low-cut-off and Warp(k) needs executing then
        continue
    else
        Warp(i).I := 0
        Pair_List[i][0] := -1 // toggling
18 if Warp(i).V == 1 and end of high cut-off epoch then
    /* Warp(i) is active */
    IRSi := VTAHit[i] / InstNo / ActiveWarpNo
    j := Interference_List[i]
    if IRSi > high-cut-off and j != i then
        if Warp(j).I == 1 then
            Warp(j).V := 0
            Pair_List[j][1] := i
        else if Warp(j).I == 0 then
            Warp(j).I := 1
            Pair_List[j][0] := i
  
```

Figure 7a) In this way, we naturally migrate data from L1D cache to shared memory, hiding the penalty of cold cache misses and coherence issues.

C. Putting It All Together

Algorithm 1 describes how CIAO schedules warps. For every low-cut-off epoch, the warp at the front of the warp list (e.g., warp i), is examined to decide whether CIAO redirects memory requests of warp i back to L1D cache or reactivate warp i . More specifically, CIAO first checks the first or second field of the *pair list* entry corresponding to warp i . Once CIAO confirms that either CIAO previously redirected memory requests of warp i to shared memory or stalled warp i because warp i severely interfered with another warp (e.g., warp k), it redirects the memory requests of warp i back to L1D cache or reactivate warp i , unless the following two conditions are satisfied: (1) IRS_k is still higher than low-cut-off and (2) warp k has not completed its execution.

Every high-cut-off epoch, CIAO examines IRS_i . If warp i is in the active warp list and IRS_i is higher than high-cut-off, CIAO looks up the *interference* list to determine which warp has most severely interfered with warp i . Once CIAO determines the most interfering warp (e.g., warp j) for warp i , CIAO checks whether it has redirected memory requests of warp j to shared memory or stalled warp j . If CIAO sees that warp j has still sent memory requests to L1D cache, it isolates warp j , redirects

# of SMs/threads	15, max 1536 per SM
L1D cache	16KB w/ 128B lines, 4 ways, write no-allocate, local write-back, global write-through, 1-cycle latency and LRU
Shared memory	48KB, 1-cycle latency and 32 banks
L2 cache	768KB w/ 128B lines, 8 ways, write allocation, write-back and LRU
DRAM	GDDR5 w/ 16 banks, tCL=12, tRCD=12, and tRAS=28
Victim tag array	8 tags per set, 48 sets, and FIFO

Table I: GPGPU-Sim configuration.

Benchmark	APKI	Input	N_{warp}	F_{smem}	Bar.	Class
ATAX [24]	64	64MB	2	0%	N	LWS
BICG [24]	64	64MB	2	0%	N	LWS
MVT [24]	64	64MB	2	0%	N	LWS
KMN [8]	46	168KB	4	1%	Y	LWS
kmeans [9]	85	101MB	2	0%	Y	LWS
GESUMMV [24]	136	128MB	2	0%	N	SWS
SYR2K [24]	108	48MB	6	0%	N	SWS
SYRK [24]	94	512KB	6	0%	N	SWS
II [8]	75	28MB	4	0%	Y	SWS
PVC [8]	64	13MB	48	33%	Y	SWS
SS [8]	34	23MB	48	50%	Y	SWS
SM [8]	140	1MB	48	1%	Y	SWS
WC [8]	19	88KB	48	1%	Y	SWS
Gaussian [9]	18	339KB	48	0%	N	CI
2DCONV [24]	9	64MB	36	0%	N	CI
CORR [24]	10	2MB	48	0%	N	CI
Backprop [9]	3	5MB	36	13%	Y	CI
Hotspot [9]	1	2MB	48	19%	Y	CI
Lud [9]	2	25KB	38	50%	Y	CI
NN [9]	8	334KB	48	0%	N	CI
NW [9]	5	32MB	48	35%	Y	CI

Table II: Benchmark characteristics. N_{warp} and F_{smem} denote the number of active warps achieving the highest performance for **Best-SWL** and the fraction of shared memory used by application running on baseline GPU.

memory requests of warp j to shared memory, and records warp i in the first field of the pair list entry corresponding to warp j to indicate that warp i has triggered to redirect memory requests of warp j . If CIAO has already redirected memory requests of warp j , then CIAO starts to stall warp j and records warp i in second field of the pair list entry corresponding to warp j . This record can be referenced when CIAO decides to reactivate warp i in future.

V. EVALUATION

A. Methodology

GPU architecture. We use GPGPU-Sim 3.2.2 [25] and configure it to model a GPU similar to NVIDIA GTX 480; see Table I for the detailed GPGPU-Sim configuration parameters [1]. Besides, we enhance the baseline L1D and L2 caches with a XOR-based set index hashing

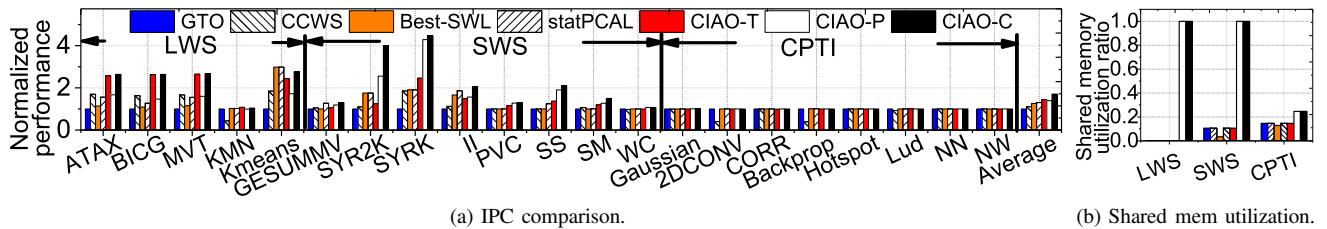


Figure 8: Performance analysis; IPC values of each warp scheduler are normalized to those of GTO.

technique [26], making it close to the real GPU device’s configuration. Subsequently, we implement seven different warp schedulers: (1) GTO (GTO scheduler with set-index hashing [26]); (2) CCWS; (3) Best-SWL (best static wavefront limiting); (4) statPCAL (representative implementation of bypass scheme [27] that performs similar or better than [6], [28]); (5) CIAO-P (CIAO with only redirecting memory requests of interfering warp to shared memory); (6) CIAO-T (CIAO with only selective warp throttling); and (7) CIAO-C (CIAO with both CIAO-T and CIAO-P). Note that CCWS, Best-SWL, and CIAO-P/T/C leverage GTO to decide the order of execution of warps. CCWS and CIAO-T/C stall a varying number of warps depending on memory access characteristics monitored at runtime. In contrast, Best-SWL stalls a fixed number of warps throughout execution of a benchmark; we profile each benchmark to determine the number of stalled warps giving the highest performance for each benchmark; see column N_{warp} in Table II.

Benchmarks. We evaluate a large collection of benchmarks from PolyBench [7], Mars [8] and Rodinia [9] which are categorized into three classes: (1) large-working set (LWS), (2) small-working set (SWS), and (3) compute-intensive (CI). Table II tabulates chosen benchmarks and their characteristics.

B. Performance Analysis

Figure 8 plots the IPC values with the seven warp schedulers and the **geometric-mean** IPC values of three benchmark classes (LWS, SWS, and CI), respectively, normalized to those with GTO. Overall, CCWS, Best-SWL, statPCAL, and CIAO-C provide 2%, 16%, 24% and 56% higher performance than GTO, respectively.

GTO performs worst among all evaluated schedulers, because, it shuffles only the order of executed warps and does not notably reduce cache thrashing caused by many active warps accessing small L1D cache. In contrast, Best-SWL outperforms GTO as it throttles some warps, reducing the number of memory accesses to small L1D and thus cache thrashing. Nonetheless, as Best-SWL must decide the number of throttled warps before execution of a given application, it cannot effectively capture the optimal number of throttled warps varying within an application compared to warp schedulers that dynamically throttle the number of

executed warps such as CCWS and CIAO. For example, as ATAX exhibits very dynamic cache access patterns at runtime, CCWS outperforms Best-SWL by 49%. Note that CCWS gives notably lower performance than Best-SWL especially for CI benchmarks; considerably affecting its performance. That is because running more active warps achieves higher performance for CI benchmarks, whereas CCWS unnecessarily stalls some active warps to give a higher priority to a few warps exhibiting high data locality. statPCAL gives up to 37% higher performance than Best-SWL by up to 37% because statPCAL offers higher TLP. Specifically, when statPCAL detects under-utilization of L2 and/or main memory bandwidth, it activates throttled warps and makes these warp directly access the underlying memory (*i.e.*, bypassing L1D cache). Due to the long access latency and limited bandwidth of underlying memory, however, statPCAL cannot significantly improve performance of LWS and SWS workloads such as KMN, SYRK, etc.

CIAO-T provides 32% and 34% higher performance than CCWS and GTO, respectively. Furthermore, CIAO-T offers 22% higher performance than Best-SWL for every benchmark except for SYR2K, II, and KMN exhibiting static cache access patterns at runtime. Both CIAO-T and CCWS dynamically stall some active warps at runtime, but our evaluation shows that it is often more effective to throttle the warps that considerably interfere with other warps than the warps with low potential of data locality as CCWS does. Furthermore, for CI benchmarks, CIAO-T offers as high performance as GTO in contrast to CCWS; refer to our earlier comparison between GTO and CCWS for CI benchmarks.

CIAO-P gives 34% higher performance than GTO. We observe that CIAO-P offers the highest TLP among all seven warp schedulers, entailing 28% higher performance than CIAO-T for SWS class benchmarks. This is because CIAO-P fully utilizes the unused space of shared memory (cf. Figure 8b). Nonetheless, its benefits can be limited for LWS class benchmarks in which the redirected memory requests of interfering warps are often too intensive and thus thrash the shared memory as well. In such a case, CIAO-T can perform better than CIAO-P, giving 48% and 66% higher performance than CIAO-P and CCWS,

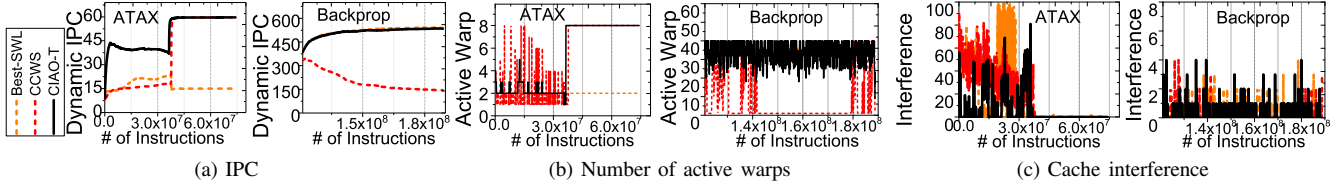


Figure 9: Comparison between Best-SWL, CCWS and CIAO-T over time: ATAX and Backprop

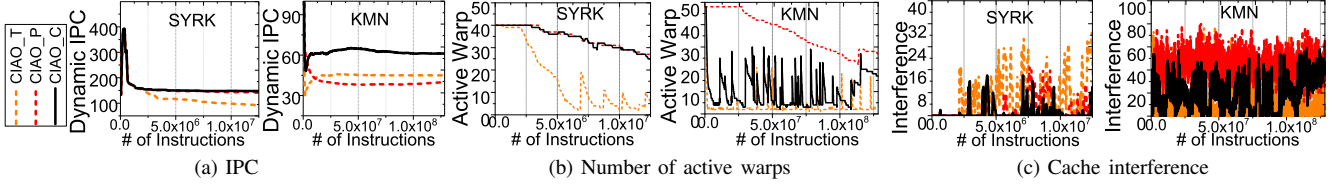


Figure 10: Comparison of CIAO-T, CIAO-P and CIAO-C over time: SYRK and KMN.

respectively, as shown in Figure 8a. Lastly, CIAO-C, which synergistically integrates CIAO-T and CIAO-P, provides 56%, 54%, 17% and 16% higher performance than GTO, CCWS, CIAO-T, and CIAO-P, respectively.

C. Effectiveness of Interference Awareness

Figure 9 shows the IPC, the number of active warps, and cache interference over time of ATAX as a representative application that exhibits distinct execution phases in a single kernel execution. For example, ATAX exhibits two distinct execution phases. The first phase comprised of the first 40-million instructions is very memory-intensive, whereas the second phase is very compute-intensive. Figure 9a shows that CIAO-T outperforms CCWS and Best-SWL for the first 40-million instructions executed. CIAO-T exhibits higher performance during this phase because CIAO-T more effectively reduces cache interference by throttling severely interfering warps, as shown in Figure 9c. After the first phase, ATAX starts a compute-intensive phase, performing the computation by fully exploiting data locality on the GPU caches. As Best-SWL cannot capture this dynamics at runtime, it executes only 2 warps for the second phase execution of ATAX. In contrast, CCWS and CIAO-C dynamically reduce the number of stalled warps as they observe

fewer cache misses and less cache interference, giving 4× higher geometric-mean performance than Best-SWL.

We choose Backprop as a representative application that is very compute-intensive but also experiences many cache misses. Figure 9 shows the performance change of Backprop over time. Best-SWL and CIAO-T provide 500 IPC on average. However, CCWS notably degrades the performance, ranging from 320 to 150 IPC because CCWS ends up giving a higher priority to warps with higher data locality and stalling more than 40 warps (or significantly reducing TLP). In contrast, CIAO-T, which offers performance similar to Best-SWL, more selectively throttles warps than CCWS (i.e., only 10~20 most interfering warps), better preserving TLP.

D. Sensitivity to Working Set Size

Small-working set. Figure 10 shows the performance of three CIAO schemes for SYRK over time. SYRK is a representative application with SWS. Specifically, Figure 10 illustrates IPC, the number of active warps, and the number of cache conflicts over time of textttSYRK over time with three CIAO schemes. As shown in Figure 10a, CIAO-P offers higher IPC than CIAO-T overall. This is because, it can secure higher TLP (*cf.* Figure 10b), whereas CIAO-T alone hurts TLP by throttling many active warps. Using the unused shared memory space, CIAO-P can effectively reduce cache interference without sacrificing TLP in contrast to CIAO-T. As expected, CIAO-C selectively stalls very few warps.

Large-working set. Figure 10 also depicts the performance of three CIAO schemes KMN, a representative application with LWS. As shown in Figure 10a, CIAO-T provides 50% higher IPC than CIAO-P, and CIAO-C always achieves the highest performance during the entire execution period amongst all three schemes. This is because, as shown

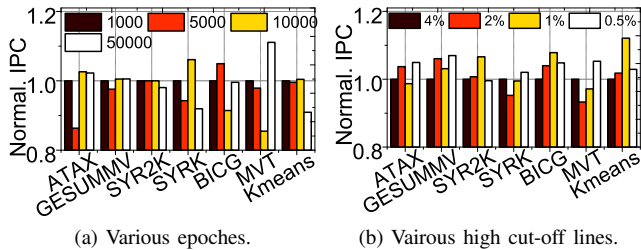


Figure 11: Sensitivity analysis.

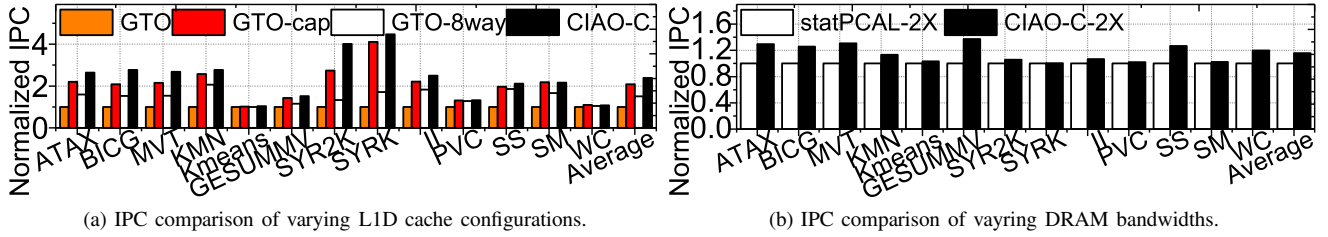


Figure 12: IPC of different L1D cache and DRAM configurations.

in Figure 10c, CIAO-P still suffers from severe shared memory interference as the amount of data requested by the partitioned warps exceeds the amount that shared memory can efficiently accommodate. In contrast, CIAO-C can better utilize shared memory by selectively throttling only the warps that cause severe interference.

E. Sensitivity Study

Epoch value. Figure 11a shows the effect of varying high-cut-off epoch values on the IPC for all the memory-intensive workloads. As we increase the epoch from 1K to 50K instructions, the change in IPC is within 15%. Note that different workloads can achieve best performance with different epoch values. That is because epoch determines the frequency of checking cache interference for CIAO. A shorter epoch provides fast response to cache interference, while a longer epoch can more accurately detect the warp causing most interference. Taking this trade-off into account, we choose 5K instructions as *high-cut-off* epoch value. An adaptive scheme can be future work.

High-cut-off threshold. Figure 11b depicts performance corresponding to different *high-cut-off* thresholds, where the *low-cut-off* threshold is fixed to half of it. All benchmarks show steady performance within 5% change during the entire execution period. This is because our CIAO throttles the active warps causing most interference, which can easily exceed the current thresholds we set. 1% is chosen in the paper.

L1D cache/DRAM configurations. Figure 12 illustrates the performance of LWS and SWS workloads by configuring various L1D cache/DRAM design parameters: (1) GTO; (2) GTO-cap (GTO but increase L1D cache capacity to 48 KB and reduce shared memory size to 16 KB); (3) GTO-8way (GTO but increase L1D cache associativity to 8 way); (4) statPCAL-2X (statPCAL but double DRAM bandwidth from 177 GB/s to 340 GB/s); (5) CIAO-C; (6) CIAO-C-2X (CIAO-C but double DRAM bandwidth). As shown in Figure 12a, while increasing L1D cache capacity (GTO-cap) and associativity (GTO-8way) can effectively improve the overall performance by 108% and 51% compared to GTO, CIAO-C still outperforms GTO-cap and GTO-8way by 14%, and 57%, respectively. This is because, GTO-cap and GTO-8way cannot fully eliminate cache interference, as

they cannot distinguish the requests between interfering and interfered warps and effectively isolate them. On the other hand, while statPCAL-2X can benefit from the increased DRAM bandwidth, bypassing requests to underlying DRAM still suffers from long DRAM delay as the latency of DRAM access is much longer than that of L1D cache access. Hence, as shown in Figure 12b, CIAO-C-2X outperforms statPCAL-2X by 16%, on average.

F. Overhead Analysis

Implementing the interference detector, CIAO leverages the VTA structure originally proposed by CCWS [12], but employs only 8 VTA entries for each warp (*i.e.*, half of the VTA entries that CCWS uses). Using CACTI 6.0 [29], we estimate that the area of one VTA structure is only 0.65 mm^2 for 15 SMs, which accounts for only 0.12% of the total chip size of NVIDIA GTX480 (529 mm^2 [30]). In addition, CIAO uses 48 registers as VTA-hit counters (one for each warp). Since each VTA-hit counter resets at the start of each kernel, a 32-bit counter is sufficient to prevent its overflow. The interference and pair lists are implemented with SRAM arrays indexed by WIDs. Since the total number of active warps in a CTA does not exceed 64 (usually, 48 active warps in each SM), we configure the interference and pair lists with 64 entries. Each entry of the interference list requires 8 (= 6+2) bits to store one warp index and saturation counter value, while each entry of pair list requires 12 (= 6 + 6) bits to store two warp indices. Using CACTI 6.0, we estimate that the combined area of the VTA-hit counters, interference list, and pair lists is 549 um^2 per SM (8235 um^2 for 15 SMs). On the other hand, Equation 1 is implemented with a few adders, a shifter, and a comparator, which also requires very low cost (2112 gates). For our shared memory modification, the translation unit, multiplexer and MSHR only need 4500 gates and 64B storage per SM. We also track the power consumption of new components employed in CIAO by leveraging GPUWattch [31], which reveals the average power is around 79mW. Overall, CIAO improves the performance by more than 50% with a negligible area cost (less than 2% of the total GTX480 chip area) and power consumption (only 0.3% of GTX480 overall power).

VI. DISCUSSION AND RELATED WORK

Warps scheduling. Several prior studies proposed to improve GPU performance by optimizing the warp scheduling methods. The two-level warp scheduler [11] statically clusters active warps into several groups and executes the warp groups with different time intervals. This approach can alleviate memory traffic by reducing the number of memory accesses. DYNCTA [32] and OWL [10] introduced data-locality aware schedulers that dynamically limit the number of active warps at runtime, which can address cache conflict problem. Similarly, DAWS [33] can predict data locality more accurately using runtime memory and branch divergence information. Unfortunately, all these schedulers do not acknowledge the cache interference exhibited by multiple active warps, are also correlated to data locality that they prioritize for warp scheduling. Further, as these schedulers throttle the active warps to address memory congestion issue, they may not be able to secure high TLP. In contrast, our CIAO monitors cache interference and partitions/throttles few thread groups that exhibit cache thrashing and interference. This allows our scheduler to remove unnecessary memory accesses, maintain higher data locality, and secure high TLP.

L1D cache and shared memory layout. There exist some GPU models such as Pascal [34] that simplify the complexity of on-chip memory design by splitting the L1D cache and shared memory into separate memory structures. While prior work [15], which proposes to flexibly partition the unified on-chip memory by users, are not compatible with these GPU models, CIAO well suits with their separate memory structure. This is because our warp partition approach introduces modified MSHR and a new address translation unit to support independent data access in shared memory.

Unbalanced cache interference. As stated in section II-B, due to the limited cache capacity, warps of regular memory access patterns can generate cache interference. Such cache interference becomes more severe and non-uniform when warps experience irregular cache access pattern. One example is GPU execution of sparse matrix-vector multiplication (SPMV), which repeatedly accesses the large and irregular sparse matrix and vector. As typical implementations [35] refer sparse matrix/vector by an index array that contains indices of non-zero data, each warp can exhibit different irregularity based on given values of the index array.

VII. CONCLUSION

In this work, we first show that warps with high potential of data locality causes severe interference at L1D cache. Then we propose to (1) redirect memory requests of such warps to unused shared memory space and (2) throttle such warps only when (1) still causes severe interference at shared memory; (2) is a completely opposite approach to CCWS which throttles warps with low potential of data locality.

Lastly, we show that the synergistic integration of (1) and (2) provides 54% higher performance than CCWS.

VIII. ACKNOWLEDGEMENT

This research is mainly supported by NRF 2016R1C1B2015312. This work is also supported in part by IITP-2017-2017-0-01015, NRF-2015M3C4A7065645, DOE DE-AC02-05CH 11231, and MemRay grant (2015-11-1731). Nam Sung Kim is supported in part by NSF 1640196 and SRC/NRC NERC 2016-NE-2697-A. Jie Zhang and Shuwen Gao contributed equally to this work. Myoungsoo Jung is the corresponding author.

REFERENCES

- [1] C. Nvidia, "Nvidia's next generation cuda compute architecture: Fermi," *Computer system*, 2009.
- [2] S. Hong and H. Kim, "An analytical model for a gpu architecture with memory-level and thread-level parallelism awareness," in *ACM SIGARCH Computer Architecture News*. ACM, 2009.
- [3] J. Lee and H. Kim, "Tap: A tlp-aware cache management policy for a cpu-gpu heterogeneous architecture," in *HPCA*. IEEE, 2012.
- [4] W. Jia, K. A. Shaw, and M. Martonosi, "Mrpb: Memory request prioritization for massively parallel processors," in *HPCA*, 2014.
- [5] M. Khairy, M. Zahran, and A. G. Wassal, "Efficient utilization of gpgpu cache hierarchy," in *GPGPU*. ACM, 2015.
- [6] Y. Tian, S. Puthoor, J. L. Greathouse, B. M. Beckmann, and D. A. Jiménez, "Adaptive gpu cache bypassing," in *Proceedings of the 8th Workshop on General Purpose Processing using GPUs*. ACM, 2015, pp. 25–35.
- [7] S. Grauer-Gray, L. Xu, R. Searles, S. Ayalasomayajula, and J. Cavazos, "Auto-tuning a high-level language targeted to gpu codes," in *Innovative Parallel Computing (InPar)*. IEEE, 2012.
- [8] B. He *et al.*, "Mars: a mapreduce framework on graphics processors," in *PACT*. ACM, 2008.
- [9] S. Che *et al.*, "Rodinia: A benchmark suite for heterogeneous computing," in *IISWC*. IEEE, 2009.
- [10] A. Jog *et al.*, "Owl: cooperative thread array aware scheduling techniques for improving gpgpu performance," *ACM SIGARCH Computer Architecture News*, 2013.
- [11] V. Narasiman *et al.*, "Improving gpu performance via large warps and two-level warp scheduling," in *MICRO*. ACM, 2011.
- [12] T. G. Rogers *et al.*, "Cache-conscious wavefront scheduling," in *MICRO*. IEEE Computer Society, 2012.
- [13] A. Bakhoda *et al.*, "Analyzing cuda workloads using a detailed gpu simulator," in *ISPASS*. IEEE, 2009.

- [15] M. Gebhart *et al.*, “Unifying primary cache, scratch, and register file memories in a throughput processor,” in *MICRO*. IEEE, 2012.
- [16] J. H. Edmondson *et al.*, “Internal organization of the alpha 21164, a 300-mhz 64-bit quad-issue cmos risc microprocessor,” *Digital Technical Journal*, 1995.
- [17] Y. Yang *et al.*, “Shared memory multiplexing: a novel way to improve gpgpu throughput,” in *PACT*. ACM, 2012.
- [18] X. Chen *et al.*, “Adaptive cache management for energy-efficient gpu computing,” in *MICRO*. IEEE, 2014.
- [19] M. K. Qureshi and Y. N. Patt, “Utility-based cache partitioning: A low-overhead, high-performance, runtime mechanism to partition shared caches,” in *MICRO*. IEEE Computer Society, 2006.
- [20] S. Srikantaiah *et al.*, “Adaptive set pinning: managing shared caches in chip multiprocessors,” in *ACM SIGARCH Computer Architecture News*. ACM, 2008.
- [21] A. B. Hayes and E. Z. Zhang, “Unified on-chip memory allocation for simt architecture,” in *SC*. ACM, 2014.
- [22] M. K. Yoon *et al.*, “Virtual thread: Maximizing thread-level parallelism beyond gpu scheduling limit,” in *ISCA*, 2016.
- [23] D. A. Jamshidi *et al.*, “D 2 ma: accelerating coarse-grained data transfer for gpus,” in *PACT*. ACM, 2014.
- [24] L.-N. Pouchet, “Polybench: The polyhedral benchmark suite,” URL: <http://www.cs.ucla.edu/~pouchet/software/polybench>, 2012.
- [25] T. Aamodt and A. Bektor, “Gpgpu-sim 3. 2: A performance simulator for many-core accelerator research,” in *ISCA*, <http://www.gpgpu-sim.org/fisca2012-tutorial>, 2012.
- [26] C. Nugteren *et al.*, “A detailed gpu cache model based on reuse distance theory,” in *HPCA*. IEEE, 2014.
- [27] D. Li *et al.*, “Priority-based cache allocation in throughput processors,” in *HPCA*. IEEE, 2015.
- [28] C. Li *et al.*, “Locality-driven dynamic gpu cache bypassing,” in *SC*. ACM, 2015.
- [29] N. Muralimanohar, R. Balasubramonian, and N. P. Jouppi, “Cacti 6.0: A tool to model large caches,” *HP Laboratories*, 2009.
- [30] NVIDIA, “NVIDIA GeForce GTX 480 <https://www.techpowerup.com/gpudb/268/geforce-gtx-480>.”
- [31] J. Leng *et al.*, “Gpuwattch: enabling energy optimizations in gpgpus,” *ACM SIGARCH Computer Architecture News*, 2013.
- [32] O. Kayiran, A. Jog, M. T. Kandemir, and C. R. Das, “Neither more nor less: optimizing thread-level parallelism for gpgpus,” in *PACT*, 2013.
- [14] NVIDIA, “Nvidia kepler next generation cuda compute architecture,” *Computer system*, vol. 26, pp. 63–72, 2012.
- [33] T. G. Rogers, M. O’Connor, and T. M. Aamodt, “Divergence-aware warp scheduling,” in *MICRO*. ACM, 2013.
- [34] NVIDIA, “Pascal GPU Architecture <http://www.nvidia.com/object/pascal-architecture-whitepaper.html>,” 2016.
- [35] B.-Y. Su and K. Keutzer, “clspmv: A cross-platform opencl smpv framework on gpus,” in *SC*. ACM, 2012.